

To appear in Proc. 4th IGPP International Astrophysics Conference,  
eds. G. Li, G. Zank and C. Russell (AIP Conf. Proc., New York)

# Diffusive Acceleration of Ions at Interplanetary Shocks

Matthew G. Baring & Errol J. Summerlin

*Department of Physics and Astronomy, MS-108, Rice University, P. O. Box 1892,  
Houston, TX 77251-1892, USA*  
Email: baring@rice.edu, xerex@rice.edu

**Abstract.** Heliospheric shocks are excellent systems for testing theories of particle acceleration in their environs. These generally fall into two classes: (1) interplanetary shocks that are linear in their ion acceleration characteristics, with the non-thermal ions serving as test particles, and (2) non-linear systems such as the Earth's bow shock and the solar wind termination shock, where the accelerated ions strongly influence the magnetohydrodynamic structure of the shock. This paper explores the modelling of diffusive acceleration at a particular interplanetary shock, with an emphasis on explaining in situ measurements of ion distribution functions. The observational data for this event was acquired on day 292 of 1991 by the Ulysses mission. The modeling is performed using a well-known kinetic Monte Carlo simulation, which has yielded good agreement with observations at several heliospheric shocks, as have other theoretical techniques, namely hybrid plasma simulations, and numerical solution of the diffusion-convection equation. In this theory/data comparison, it is demonstrated that diffusive acceleration theory can, to first order, successfully account for both the proton distribution data near the shock, and the observation of energetic protons farther upstream of this interplanetary shock than lower energy pick-up protons, using a single turbulence parameter. The principal conclusion is that diffusive acceleration of inflowing upstream ions can model this pick-up ion-rich event without the invoking any seed pre-acceleration mechanism, though this investigation does not rule out the action of such pre-acceleration.

## INTRODUCTION

Evidence for efficient particle acceleration at collisionless shocks in the heliosphere abounds, including direct measurements of accelerated populations in various energy ranges at the Earth's bow shock (e.g. [1, 2]) and interplanetary shocks (for the pre-Ulysses era see, for example, [3, 4, 5]). The development of theories of shock acceleration is therefore strongly motivated, and a variety of approaches have emerged. One possible means for the generation of non-thermal particles is the Fermi mechanism, often called diffusive shock acceleration; this process forms the focus of this paper.

There are various approaches to modelling diffusive shock acceleration. Among these are hybrid and full plasma codes (e.g. [6, 7, 8, 9]), which place an emphasis primarily on plasma structure and wave properties in the environs of shocks, and the convection-diffusion differential equation approach [10]. In addition, the kinematic Monte Carlo technique of Ellison and Jones (e.g., [11, 12, 13]) also focuses on diffusion and convection, and describes the injection and acceleration of particles from thermal energies to the highest relevant energies, addressing both spectral and hydrodynamic properties. The simulation technique makes no distinction between accelerated particles and ther-

mal ones, using an identical phenomenological description of diffusion for both. In this work, following previous invocations, it is assumed that a particle's mean free path  $\lambda$  is proportional to its gyroradius  $r_g$ , i.e.  $\lambda = \eta r_g$ , with  $\eta = \text{const.}$  for all particle momenta. Upstream plasma quantities are input from observational data, and downstream quantities are determined using the full MHD Rankine-Hugoniot relations.

The Monte Carlo technique was used by Ellison et al. [14] to perform the first detailed theory/data comparison for the quasi-parallel portion of the Earth's bow shock. They compared predictions of the Monte Carlo method with particle distributions of protons,  $He^{++}$  and a  $C$ ,  $N$  and  $O$  ion mix obtained by the AMPTE experiment. The agreement between model predictions and data was impressive, but required modeling in the non-linear acceleration regime, when the dynamic effects of the accelerated particles control the shock structure. A similar theory/data comparison was explored for interplanetary (IP) shocks in the work of Baring et al. [15], where impressive agreement was found between the Monte Carlo predictions and spectral data obtained by the Solar Wind Ion Composition Spectrometer (SWICS) aboard Ulysses, in the case of two shocks observed early in the Ulysses mission. Such agreement was possible only with the assumption of strong particle scattering (i.e. near the Bohm diffusion limit) in the highly oblique candidate shocks. For a third shock, detected a month later, the comparison failed with significant differences arising in the 500-800 km/sec range of the phase space distribution. Baring et al. [15] attributed this discrepancy to the omission of pick-up ions from the model: such an extra component would be expected to provide a substantial contribution to the accelerated population in this particular event.

This paper explores the role of pick-up ions in such shocks via modeling the accelerated population for the specific IP shock detected by the SWICS and HI-SCALE instruments aboard the Ulysses spacecraft at around 4.5 AU, as reported in [16]. Phase space distributions from the simulations are compared with SWICS and HI-SCALE data, yielding acceptable fits for the proton populations using standard prescriptions for the injected pick-up ion distribution. The simulation results successfully account for the observation of energetic protons farther upstream of the forward shock than lower energy pick-up protons, since a rigidity-dependent diffusion is used in the modeling.

## THE ULYSSES EVENT OF DAY 292, 1991

The forward shock of a CIR encountered by Ulysses on Day 292 of 1991, is appropriate for a case study, with downstream particle distributions published in Gloeckler et al. [16]. Various plasma parameters for this shock were input for the Monte Carlo simulation, and were obtained from [16] and the data compilations of [17, 18]. The shock was quite oblique, with  $\theta_{Bn1} = 50^\circ \pm 11^\circ$  being the angle the upstream magnetic field made with the shock normal. It was also quite weak, with a sonic Mach number of  $M_s \sim 2.53$ , and [16] inferred a value of  $r = u_1/u_2 = 2.4 \pm 0.3$  for the velocity compression ratio. The normalization of solar wind proton distributions was established using  $n_p = 2.0 \text{ cm}^{-3}$  as the solar wind proton density. Other parameters, such as the fluid speeds and upstream plasma temperatures, are detailed in Summerlin & Baring [19], yielding an upstream flow speed of  $u_1 \approx 55 \text{ km/s}$  in the shock rest frame. The pick-up proton distribution

input for the Monte Carlo simulation was taken from [20], a developed expression that is modeled on the seminal work of [21], and is similar in conception to pick-up ion distributions used in [22]. The pick-up ion model provides both the detailed shape and normalization of this superthermal distribution at 4.5AU; it incorporates the gravitational focusing of interstellar neutrals, the physics of their ionization as a function of distance from the sun, and adiabatic losses incurred during propagation away from the sun.

The Monte Carlo shock acceleration simulation is described in [12, 13, 15, 19]. Particles are injected upstream and allowed to convect into the shock, meanwhile diffusing in space so as to effect multiple shock crossings, and thereby gain energy through the shock drift and Fermi processes. The particles gyrate in laminar electromagnetic fields, with their trajectories being obtained by solving the Lorentz force equation in the shock rest frame, in which there is, in general, a  $\mathbf{u} \times \mathbf{B}$  electric field in addition to the magnetic field. The effects of magnetic turbulence are modeled by scattering these ions in the rest frame of the local fluid flow. While the simulation can routinely model either large-angle or small-angle scattering, in this paper, large-angle scattering is employed, appropriate for the turbulent fields in IP shocks. For this phenomenological scattering, it is assumed that a particle's mean free path  $\lambda$  is proportional to its gyroradius  $r_g$ , i.e.  $\lambda = \eta r_g$ , with  $\eta = \text{const.}$  for all particle momenta. Other dependences on particle rigidity can be employed, however the results are not extremely sensitive to such choices.

At every scattering, the direction of the particle's momentum vector is randomized in the local fluid frame, with the resulting effect that the gyrocenter of a particle is shifted randomly by a distance of the order of one gyroradius in the plane orthogonal to the local field. Accordingly, cross-field diffusion emerges naturally from the simulation, and is governed by a kinetic theory description [13, 23], where the ratio of the spatial diffusion coefficients parallel ( $\kappa_{\parallel} = \lambda v/3$ ) and perpendicular ( $\kappa_{\perp}$ ) to the mean magnetic field is given by  $\kappa_{\perp}/\kappa_{\parallel} = 1/(1 + \eta^2)$ . Clearly then,  $\eta$  couples directly to the amount of cross-field diffusion, and is a measure not only of the frequency of collisions between particles and waves, but also of the level of turbulence present in the system, i.e. is an indicator of  $\langle \delta B/B \rangle$ . The Bohm diffusion limit of quasi-isotropic diffusion, presumably corresponding to  $\langle \delta B/B \rangle \sim 1$ , is realized when  $\eta \sim 1$ . As will become apparent,  $\eta$  is a parameter that critically controls the injection efficiency of low energy particles, and the upstream diffusion scale of accelerated ions. The simulation outputs particle fluxes and phase space distributions at any location upstream or downstream of the shock, and in any reference frame including that of the Ulysses spacecraft. This capability renders it ideal for comparison with observational data.

Figure 1 displays downstream distributions for thermal, pick-up and accelerated protons from the Monte Carlo simulation and the SWICS and HI-SCALE measurements (see Fig. 1 of [16]) taken in the frame of the spacecraft on the downstream side of the Day 292, 1991 shock. The solar wind and pick-up proton parameters are fairly tightly specified, so that the model has one largely free parameter, the ratio of the particle mean free path to its gyroradius,  $\eta = \lambda/r_g$ . The efficiency of acceleration of thermal ions in oblique shocks, i.e. the normalization of the non-thermal power-law, is sensitive [13, 15] to the choice of  $\eta$ , so this parameter was adjusted to obtain a reasonable “fit” to the data. Here, the accelerated pick-up ion phase space density is about a factor of 30 greater than that of the solar wind ions, denoted in the figure by the “SW only” histogram.

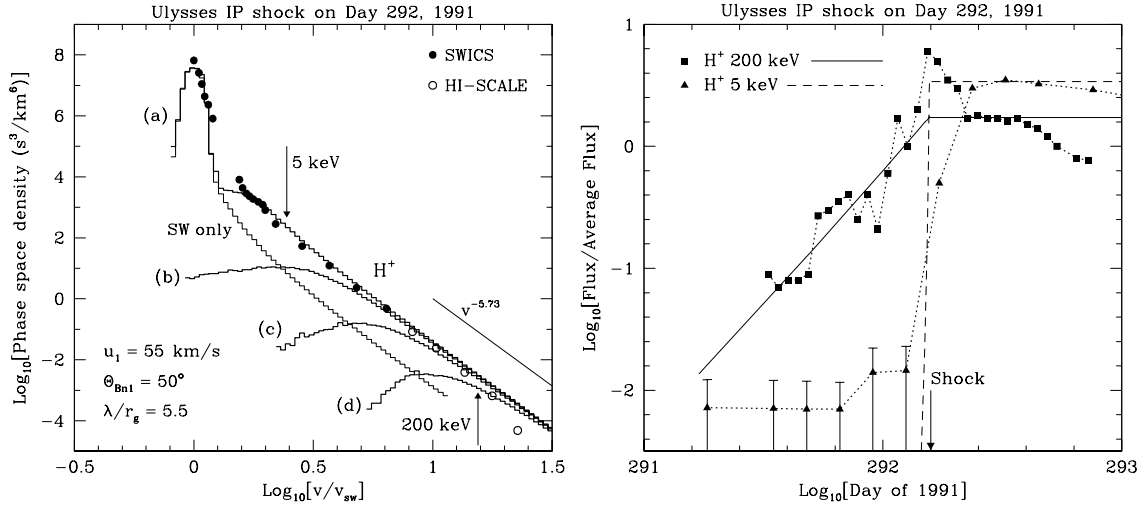


**FIGURE 1.** *Left panel:* Comparison between phase space velocity distribution functions for data collected by the Ulysses mission for the shock on day 292 of 1991, and Monte Carlo model results. The data are for  $H^+$  (filled circles for SWICS data; open circles for HI-SCALE points) solar wind and pickup ions, and are taken from Gloeckler et al. [16]. The heavyweight histograms are the corresponding Monte Carlo models of acceleration of protons for  $u_1 = 55$  km/sec, using the optimal choice of plasma shock parameters from [16] and sources indicated in the text (see also [19]). These four spectra correspond to (a) downstream, and successively increasing times upstream of the shock encounter, i.e. (b) 14 minutes, (c) 69 minutes and (d) 278 minutes upstream. The lighter weight histogram marked “SW only” was for a run where pick-up ions were omitted. The velocity axis is the ratio of the ion speed  $v$ , as measured in the spacecraft frame, to the solar wind speed. The model assumed  $\eta = \lambda/r_g = 5.5$  and a shock of compression ratio  $r = 2.1$ , corresponding to diffusive acceleration power-laws of index  $-5.73$ , is indicated.

*Right panel:* The flux variations of accelerated pick-up ion populations as a function of time near the shock. The data for 5 keV and 200 keV pick-up  $H^+$  are depicted by filled triangles and squares, respectively, and are taken from [16]. The Monte Carlo model generated fluxes at different distances normal to the shock, and were converted to spacecraft times by incorporating solar wind convection. The 5 keV and 200 keV pick-up  $H^+$  traces are displayed as dashed and solid curves, respectively, and exhibit an exponential decline upstream of the shock that is characteristic of diffusive shock acceleration.

The downstream fit in the left hand panel of Fig. 1 models the accelerated protons well, for  $\eta = 5.5 \pm 1.5$ , a value that is slightly higher than those inferred in the fits of [15] for shocks at around 2–3 AU, yet consistent with a moderate level of field turbulence. The uncertainty in the inferred value of  $\eta$  is due mostly to the observational uncertainty in the shock obliquity  $\theta_{Bn1}$ . The non-thermal proton distribution is composed virtually entirely of accelerated pick-up ions: the accelerated thermal  $H^+$  ions are injected much less efficiently in the simulation than in the observations. The efficiency of acceleration of thermal ions could be increased via several means: (i) by lowering the shock obliquity angle  $\theta_{Bn1}$ , for which there is a large observational uncertainty; (ii) by decreasing  $\eta$ , corresponding to increased turbulence, without altering the pick-up ion acceleration efficiencies substantially, and (iii) increasing the temperature of the thermal ions somewhat, though this would reduce the compression ratio and accordingly steepen the non-thermal continuum. Note that the distribution of accelerated  $He^+$  pick-

up ions reported by [16] for this shock can be modeled by the *same* scattering parameter  $\eta = 5.5$ . This enticing property is addressed by Summerlin & Baring [19], where it is observed that the  $He^{++}$  distribution requires lower  $\eta$  for a fit of comparable quality.

An instructive diagnostic on the acceleration model is to probe the spatial scale of diffusion. This is routinely performed with the Monte Carlo simulation by placing flux measurement planes upstream of the shock at different distances, as well as downstream. Results are illustrated in the left hand panel of Fig. 1 via the display of upstream distributions of high energy particles at different times, i.e. distances from the shock. The Figure exhibits the characteristic “peel-off” effect where superthermal ions become depleted at successively high energies the further the detection plane is upstream of the shock; this signature was first identified by Lee [24]. Gloeckler et al. [16] discussed an energy-dependent rise in fluxes of non-thermal particles *prior* to the shock crossing. This was cited as indicating the existence of a pre-acceleration mechanism. Fluxes for two different  $H^+$  ion energies, 5 keV and 200 keV, were obtained from spectra like those in the left hand panel in the Fig. 1, and are displayed in the right hand panel of the Figure, together with corresponding data from Fig. 3 of [16] for identical energy windows. Note that the Ulysses data normalization was established by averaging over 3 days of data, whereas the model normalization was adjusted to match observed fluxes around 1/2 day downstream of the shock.

It is clear that the spatial scale of the exponential decline of ions upstream of the shock is more or less identical to that of the model, for our choice of  $\eta = 5.5$ . High energy particles with a mean free path  $\lambda \propto r_g$  establish an exponential dilution in space/time due to random scattering of the particles as they leak upstream against a convective flow. For the 200 keV ions with their relatively long mean free paths, the simulation results are clearly well correlated with the data prior to the shock, modulo plasma fluctuations, and in particular the overshoot just downstream. On the other hand, for the lower energy 5keV ions, the exponential decay has a very short time scale, around a factor of 40 smaller than for the 200 keV ions, realizing background levels upstream until very close to the shock. So, although the simulation results are consistent with the observed results, it is impossible to draw more definitive conclusions without an improvement in data time resolution, or a focus on ions of intermediate energy, say around 50 keV. Note that while this comparison is suggestive, it does not conclusively prove that diffusion is the dominant operating mechanism in this system. Yet alternative explanations must generate exponential declines that are consistent with convective loss scales of the order of a few gyroradii, with the physical mechanism responsible for transport upstream being also a direct cause of injection into the acceleration process.

## CONCLUSIONS

This paper has compared the phase space distributions for protons from the Monte Carlo simulation of diffusive shock acceleration with those observed by the Ulysses instruments SWICS and HI-SCALE in the Day 292, 1991 shock. There is a good deal of consistency between theory and experiment for the energetic protons above speeds around 600 km/sec, an agreement that is extended to include  $He^+$  pick-up ion spectra

in [19]. At these speeds, the injection of pick-up protons dominates that of solar wind protons. The normalization of the energetic proton power-law establishes  $\eta = 5.5$ , where  $\lambda = \eta r_g$  is the diffusive mean free path. This provides substantial cross-field diffusion ( $\kappa_{\perp}/\kappa_{\parallel} \approx 0.03$ ), the prerequisite for efficient injection and acceleration in this diffusive model, when highly oblique shocks are being simulated.

The upstream spatial scales of the acceleration were also probed, with the flux increases of energetic protons seen upstream of the shock being well-modeled by the expected upstream “leakage” associated with diffusive acceleration. The value of  $\eta = 5.5$  inferred from the spectral fit scales the upstream diffusive lengthscale, and the accompanying exponential decline in predicted flux is commensurate with the Ulysses data presented in Gloeckler et al. [16]. Hence, the observed upstream flux precursor is not clear evidence of a pre-acceleration mechanism, as claimed by [16], though it is quite possible that some pre-acceleration mechanism may be acting. The flux fluctuations in time clearly indicate the contribution of a non-diffusive process in the plasma shock, effects that are not incorporated in the simulation. Yet, the fact that the diffusive model works so well in coupling the spectral and spatial properties suggests that diffusion is an integral part of the acceleration process at this shock.

## REFERENCES

1. Scholer, M., Ipavich, F. M., Gloeckler, G., & Hovestadt, D. 1980, J. Geophys. Res. 85, 4,602.
2. Gosling, J. T., Thomsen, M. F., Bame, S. J., & Russell, C. T. 1989, J. Geophys. Res. 94, 3555.
3. Sarris, E. T., & Van Allen, J. A. 1974, J. Geophys. Res. 79, 4,157.
4. Decker, R. B., Pesses, M. E., & Krimigis, S. M. 1981, J. Geophys. Res. 86, 8819.
5. Tan, L. C., Mason, G. M., Gloeckler, G., & Ipavich, F. M. 1988, J. Geophys. Res. 93, 7,225.
6. Quest, K. B. 1988, J. Geophys. Res. 93, 9,649.
7. Winske, D., Omid, N., Quest, K. B. & Thomas, V. A. 1990, J. Geophys. Res. 95, 18,821.
8. Giacalone, J., Burgess, D., & Schwartz, S. J. 1992, in *Study of the Solar-Terrestrial System*, (ESA Special Publication, Noordwijk) p. 65.
9. Kucharek, H. & Scholer, M. 1995, J. Geophys. Res. 100, 1,745.
10. Kang, H., & Jones, T. W. 1995, ApJ 447, 944.
11. Ellison, D. C., Jones, F. C. & Eichler, D. 1981, J. Geophys. - Zeitschrift fuer Geophysik, 50, 110.
12. Jones, F. C. & Ellison, D. C. 1991, Space Sci. Rev. 58, 259.
13. Ellison, D. C., Baring, M. G. & Jones, F. C. 1995, ApJ 453, 873.
14. Ellison, D. C., Möbius, E., & Paschmann, G. 1990, ApJ 352, 376.
15. Baring, M. G., Ogilvie, K. W., Ellison, D., & Forsyth, R. 1997, ApJ 476, 889.
16. Gloeckler, G., Geiss, J., Roelof, E. C., et al. 1994, J. Geophys. Res. 99, 17,637.
17. Balogh, A., et al. 1995, Space Sci. Rev. 72, 171.
18. Hoang, S., et al. 1995, Adv. Space Res. 15 (8/9), 371.
19. Summerlin, E. J. & Baring, M. G. 2005, Adv. Space Res. in press. [astro-ph/0505569]
20. Ellison, D. C., Jones, F. C. & Baring, M. G. 1999, ApJ 512, 403.
21. Vasyliunas, V. M., & Siscoe, G. L. 1976, J. Geophys. Res. 81, 1247.
22. le Roux, J. A., Potgieter, M. S., & Ptuskin, V. S. 1996, J. Geophys. Res. 101, 4,791.
23. Forman, M. A., Jokipii, J. R. & Owens, A. J. 1974, ApJ 192, 535.
24. Lee, M. A. 1982, J. Geophys. Res. 87, 5063.